Evaluation of the protective role of ellagic acid in retinal degeneration: an experimental model

Eman E. Mousa[a], Aziza A. Elsaied[a], Mohammad M. Murad[b], Amal E. Ibrahim[c]

[a]Department of Biophysics, Faculty of Science, Alazhar University, Cairo, [b]Departments of Ophthalmology, [c]Visual Science, Research Institute of Ophthalmology, Giza, Egypt

Correspondence to Amal E. Ibrahim, PhD, Department of Visual Science, Research Institute of Ophthalmology, Giza POX: 90, Egypt. Tel: 01002551234; e-mail: amalawady@hotmail.com

Received: 1 September 2024
Revised: 29 September 2024
Accepted: 3 October 2024
Published: 24 December 2024

Journal of The Arab Society for Medical Research 2024, 19:211–220

Background/aim
Ellagic acid (EA) is widely recognized as a natural compound with pharmacological potency as a polyphenolic molecule, possessing antioxidant, anti-inflammatory, antimutagenic, and antiproliferative characteristics. The present study aims to evaluate the potential neuroprotective effect of EA in retinal degeneration induced experimentally in rabbits.
Material and methods
A total of 27 male white New Zealand rabbits, with an average weight ranging from 1.5 to 2 kg, were divided into three groups (nine each). Group I served as the control group, while group II and group III, the macular degeneration (MD) induction groups that received a single intravitreal injection of sodium iodate (SI). Following the injection, group III was given 50 mg/kg of EA powder for 21 days, starting immediately after MD induction. Ophthalmic examinations of the retinas were conducted on days 7, 14, and 21 using a fundus camera, followed by electroretinogram (ERG) recording after MD induction. Apoptotic caspase-3 and caspase-7 activities in the retina tissues were also measured postdecapitation.
Results
The results showed a significant decrease ($P \leq 0.05$) in electroretinogram 'a- and b-waves' following intravitreal SI injection in group II and III comparing with control group. The pattern of internucleosomal fragmentation, indicating apoptosis, was time-dependent. The injection also increased relative caspase-3 and caspase-7 activity. However, group III of rabbits that is treated with EA exhibited noticeable improvements in these outcomes in comparing with group of MD-induced rabbits.
Conclusions
The administration of EA demonstrated a notable impact in improving the retina's function, and decreased the apoptosis levels in MD model of rabbits

Keywords:
apoptosis, electroretinogram, ellagic acid, sodium iodate, rabbit, retina

J Arab Soc Med Res 19:211–220

1687-4293

Introduction

Retinal neurodegenerative diseases, including the prevalent macular degeneration (MD), have become a growing concern on a global scale. The incidence of this disease is increasing and shows global variation. The prevalence of retinal neurodegenerative diseases, including MD, is rising worldwide and demonstrates significant geographical variations in incidence rates. This growing trend is raising concerns globally [1]. Projections estimate that the global population of individuals diagnosed with MD is anticipated to reach approximately 288 million by the year 2040 [2]. The neurodegenerative process associated with MD results in permanent neuronal damage to the retina, thus being the main contributor to progressive visual impairment.

Oxidative stress is a phenomenon characterized by the impairment of cellular or molecular structures due to the presence of reactive oxygen species (ROS). This phenomenon is particularly prevalent in age-related ailments, arising from an imbalance between the generation of ROS and the protective antioxidant defense mechanism [3]. Considering the lack of existing treatment to counteract the degeneration and neuronal loss in the retina, the implementation of supplementary or supportive therapies is advantageous.

Antioxidants are chemical compounds that interact with free radicals, neutralizing their harmful effects and impeding potential damage. Antioxidants are commonly known as 'free radical scavengers' in academic literature [4,5]. A diet rich in antioxidants, vitamins, and minerals has the potential to mitigate the likelihood of MD advancement [6]. The concept that the utilization of antioxidants is advantageous in models of ocular diseases induced by oxidative stress is supported by preclinical and clinical investigations. The Mediterranean and Oriental diets, which are naturally rich in antioxidants, have demonstrated efficacy in the prevention or deceleration of age-related macular degeneration (AMD) in patients [7]. The primary objective for elderly patients is the prevention of age-related issues.

Ellagic acid (EA) is a bioactive polyphenolic molecule found naturally as a secondary metabolite in several plant species. EA is found in significant concentrations in pomegranate (*Punica granatum L.*) and several fruit varieties [8]. The substance in question has been recognized for its antioxidant properties, which safeguard against the detrimental impacts of free radicals. EA has diverse therapeutic activities, alongside its pharmacological potential, for treating many diseases and disorders. Numerous studies have demonstrated the efficacy of this intervention in mitigating the risk of cardiovascular and neurological disorders, cancer, and diabetes [9]. The word 'EA' has been utilized as the principal topic, with a special emphasis on academic publications released in the last ten years [10].

Zhipeng *et al.* [11] developed noninvasive liposomes (EA-Hb/TAT and isoDGR-Lipo) to efficiently co-deliver EA and oxygen to prevent retinal cell apoptosis. EA reduced the abnormalities in the retina. It attenuated the retinal abnormalities including electroretinogram (ERG) and apoptosis [12].

To examine diseases of the retinal pigment epithelium (RPE) and photoreceptors, it is necessary to employ experimental animal models for retinal degeneration [13]. The induction of retinal degeneration in rabbits with $NaIO_3$ is a commonly employed method for investigating cellular apoptosis in MD. The outcome of this phenomenon is the demise of retinal pigmented epithelium, which is then followed by the secondary demise of photoreceptors, akin to the observed pattern in Geographic Atrophy [14].

The present study aims to investigate, whether the consumption of EA can slow down the progression of MD and evaluate its potential neuroprotective effect in rabbits' retinas.

Materials and methods

Animals

This investigation utilized a sample of 27 male New Zealand white rabbits, with each rabbit weighing between 1.5 and 2 kg. The animals were maintained in distinct enclosures within the animal house facility of the (RIO), under the supervision of veterinary personnel. They were kept under standard settings of temperature and humidity, with a temperature range of 22±2°C, humidity levels between 45 and 55%, and a light intensity of 300–400 lux. The rabbits were provided with regular feed and unrestricted access to water while housed in an environment with a 12 h dark/light cycle.

Retinal MD induction

The retinal MD induction in rabbits was done using freshly generated sterile sodium iodate (SI) solutions that were prepared at a concentration of 16 mg/ml. This was achieved by dissolving solid SI powder (S4007, Sigma-Aldrich, St. Louis, MO, USA) in 0.9% normal saline. A combination of tiletamine hydrochloride/zolazepam hydrochloride (15 mg/kg; Zoletil, Virbac, Carros, France) and xylazine hydrochloride (0.2 ml/kg; Rompun, Bayer Corp., Shawnee Mission, KA, USA) was utilized to induce anesthesia in the rabbits. A diluted povidone-iodine solution and topical proparacaine hydrochloride (Alcaine, Alcon Laboratories, Inc., Fort Worth, TX, USA) were applied to the eye before injection. Eighteen rabbits were injected using a 30-gauge needle syringe, and 0.01 µl of SI solution corresponding to 0.8 mg was intravitreally injected. The right eye was injected once with SI solution 2 mm posterior to the limbus. The injected eyes were subjected to a daily administration of topical fluoroquinolone solution for a maximum duration of 3 days following the injection. No injections were administered to the left eye [15].

Administration of Ellagic acid

After SI injection, nine rabbits were randomly selected and 50 mg/Kg of EA (E2250, Sigma-Aldrich, ≥95% (HPLC), powder, from tree bar St. Louis, MO, USA) orally daily for 21 days.

Ethical consideration

All the experiments were done in compliance with the Public Health Guide for the care and use of laboratory animals and adhering to the guidelines set forth by The Association for Research in Vision and Ophthalmology. The present protocol has been approved by the local Ethical Committee of the Research Institute of Ophthalmology in Giza, Egypt (RIO), with approval number FWA0031869.

Study design

The rabbits were allocated into three groups (nine each) using a random allocation method.

Group I: The control group remained untreated.

Group II: MD-induced rabbits that received a single intravitreal injection of sodium iodate (SI) [15].

Group III: MD-induced rabbits that received a single intravitreal injection of SI and were given 50 mg/kg of EA powder daily for 21 days.

All rabbits of the three groups included in this study were subjected to the following measurements after certain induction periods, namely 7, 14, and 21 days.

Fundus photography

To investigate observable anatomical retinal alterations, the fundi were analyzed by employing a Super Quad 160 lens (manufactured by Volk Optical, Inc., located in Mentor, OH, USA). This lens was placed over the cornea after phenylephrine hydrochloride and tropicamide drops were applied to the ocular surface.

Mydrin-P, developed by Santen in Osaka, Japan, induces optimal pupillary dilation. A digital camera (D60, Nikon Corp., Tokyo, Japan) was used to obtain colour fundus images from all eyes.

Electroretinography

Baseline standards for ERG were established using the Neuro-ERG device produced in Russia by Neurosoft Medical Diagnostics at the Research Institute of Ophthalmology in Giza, Egypt. ERGs of a monocular flare were obtained from right eyes. For intramuscular anesthesia, the animals were administered 0.1 ml/kg of separine and 50 mg/kg of ketamine hydrochloride. The rabbits were then subjected to a period of dark adaptation lasting a minimum of 30 min, following pupillary dilatation achieved with the application of topical 1% mydriacyl. The animals were then positioned on the surgical table's surface under controlled and sustained body temperatures of 37°C. Each rabbit was precisely positioned with their head inclined to one side before being administered topical anesthetic eye drops. The active electrode, shaped like a hook, was positioned on the lower eyelid. The earthed electrode was placed on the earlobe opposite the eye being examined, while the reference electrode was placed on the earlobe adjacent to the eye being examined. The ERG data was filtered using a low-pass filter with a cutoff frequency of 300 Hz and a high-pass filter at 0.3 Hz [16]. ERGs were conducted in accordance with the standard protocol the International Society for Clinical Electrophysiology of Vision. The scotopic 3.0 protocol was employed to elicit the maximal combined response of rods and cones. A flash intensity of 3.007 cd/m^2 lasting for duration of 0.5 ms, was utilized for the ERG measurements [17]. All assessments were conducted under standard room temperature conditions, and no signs of rapid breathing were present.

Apoptosis

DNA fragmentation studies by gel electrophoresis

The rabbits were decapitated, and then their eyes were removed via enucleation. Subsequently, the eyes were opened by making a corneal section along the ora serrata. After removing the corneas, the iris was then extracted using forceps, facilitating the concurrent removal of the eye lens and vitreous humour. The retina-containing eye cub was sectioned into blocks for DNA extraction and frozen in liquid nitrogen. The tissue sample was carefully placed in a sterilized, DNAase- and RNase-free container. 40 μl of 10% SDS solution and 4 μl of 20 mg/ml proteinase K were added to each tissue sample. After that, the samples were incubated overnight at 55°C in a hybridization oven. Each sample was treated with 175 μl of buffered phenol and 175 μl of chloroform/isoamyl (24 : 1) before being subjected to centrifugation at 15 000 rpm for 20 min. The liquid phase was transferred to a microtube that had been sterilised. An aliquot of chloroform/isoamyl (24 : 1) was introduced into the supernatant in a volume corresponding to the supernatant obtained in the preceding step. The liquid was held in new microtubes and centrifugated at 15 000 rpm for 20 min. To each sample, 10 μl of RNase was added and incubated at 37°C for 1 h. To match the supernatant volume, chloroform/isoamyl (24 : 1) was added. After that, the mixture was centrifuged again at 15 000 rpm for 20 min. A volume of 250 μl of each supernatant was carefully transferred into a fresh microtube with care. Subsequently, 7.5 μl of a 5 M NaCl solution was added to the supernatant, resulting in a final concentration of 0.15 M NaCl in the sample. The samples were inverted and mixed gently. An equal volume of supernatant of −20°C and 100% ethanol was added. Samples were gently blended by inversion. DNA had a filamentous precipitated morphology. The DNA precipitate was visually identified and centrifuged at 15 000 rpm for 20 min. The supernatant was carefully pipetted away, retaining the DNA pellets. If visible DNA pellets were present, the solution was stored at −20°C for a long time, centrifuged, and the supernatant was removed while the solid DNA pellets were retained. Next, 500 μl of −20°C 70% ethanol was added into DNA pellets.

The mixture tube was gently inverted several times and centrifuged at 15 000 rpm for 20 min at 0°C. After carefully pipetting out the solution, the DNA pellets were preserved in the microtube. The microtubes were exposed in an open fume hood for 15–20 min to evaporate ethanol. Then, the pellet was reconstituted in 75 µl of sterilized distilled water or Tris-EDTA (TE) buffer. Subsequently, the pellet was allowed to reconstitute overnight at room temperature under the fume hood. The DNA concentration was determined using a spectrophotometer (Bio-Rad UV Transilluminator 2000 Bio-Rad USA).

Caspase-3 and caspase-7 activity assay

According to the manufacturer's instructions, caspase-3 and caspase-7 levels were determined in the soluble fraction of retina tissue homogenate using double-sandwich ELISA Kits for rabbits by Bioassay Technology Laboratory, Cat.NO.E0324Rb and My BioSource, Cat.NO.MBS034908 respectively. Protein levels in the samples were assessed using a colourimetric method of BCA Protein Assay Kit (Elabscience, Cat.NO.E-BC-K075-S) by Microplate Reader RT-2100C_ELISA READER Brand: Meditech USA.

Statistical analysis

Data analysis was performed using SPSS version 23.0 (IBM SPSS Statistics for Windows, Version 23.0. Armonk, NY: IBM Corp; USA). Data of Bands was presented as number and percentage of bp fragmentation for ladder and different groups, while the quantitative data was presented as mean±SD (stander deviation) and analyzed using one-way analysis of variance method to examine the electroretinographic measurements and assess the number of apoptotic cells or the activity of caspases. If the analysis of variance was significant, subsequent multiple comparisons were conducted to ascertain the specific pairs of mean values that exhibited significant differences. The post hoc Newman–Keuls test evaluated the significant differences between groups. The predetermined significance level was established at *P* less than 0.05.

Results

Fundus

For control eyes, no abnormalities were found in fundi throughout the follow-up period (Fig. 1a). In the second and third groups, photographs revealed retinal vascular attenuation and atrophy starting to be noted from the first follow-up on the 7th day and gradually progressive in the next follow-ups (Fig. 1b & c). In all follow-ups, no abnormality was noted in the anterior segment. All rabbits showed normal behaviour and activity without any significant weight loss.

Functional changes on ERG

Figure 2 illustrates the ERG responses of the dark-adapted eyes for all groups, while Table 1 shows the mean and standard deviation of the amplitude of both a- and b-waves for ERG in all groups.

An ERG of a control rabbit (group I) showing normal peaks for both the (a and b) –waves. The a-wave amplitude and implicit time had mean values of 26.1 ±1.81 µV and 13.26±0.92 m sec, respectively. The b-wave exhibited mean values of 54.8±1.81 µV and 34 ±0.69 m sec. The amplitudes were determined by calculating the distance between the baseline and the lowest point of the negative peak for the a-wave and from this minimum point to the positive peak for the b-wave.

Figure 1

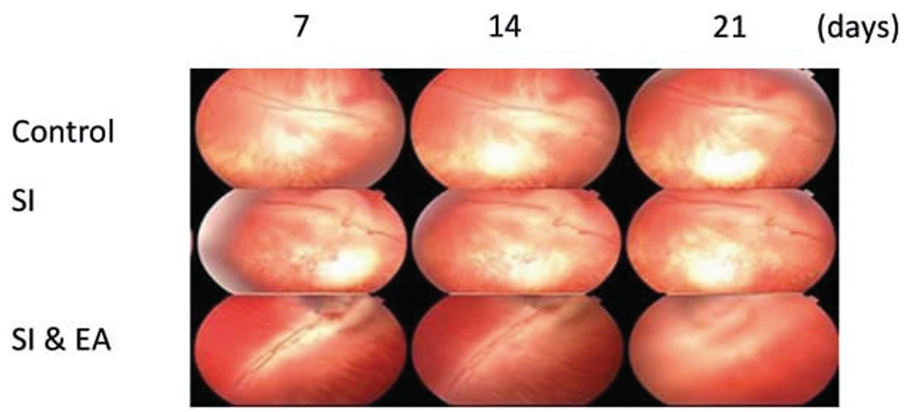

Sequential fundus photographs at days 7, 14, and 21 of rabbit's retina. (a) Control group, (b) Group received sodium iodate (SI) and (c) Group received SI and was treated with ellagic acid (EA).

Figure 2

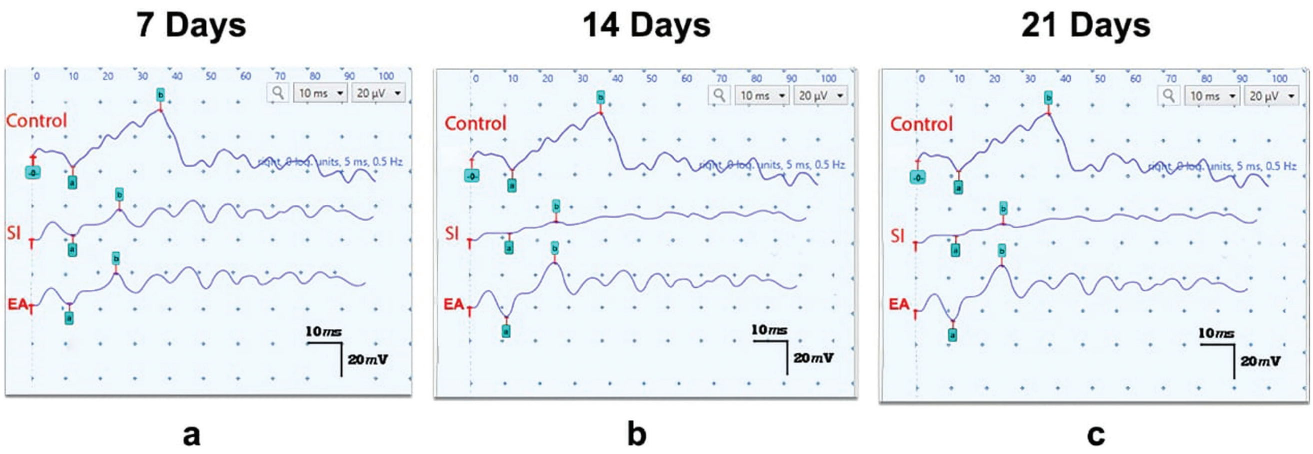

Typical records of electroretinogram for rabbit's control, injected with sodium iodate (SI) and group of rabbits that injected with SI and treated with ellagic acid (EA), after 7 (a), 14 (b) and 21 (c) days.

The second experimental group, which was administrated with SI (group II), showed a significant reduction in the amplitude of both a- and the b-waves on the seventh day ($P<0.05$). There is also a delay in the implicit time of both waves. Furthermore, there was a significant decline in a- and b-wave amplitudes during the trial, which spanned 21 days. The a- and b-wave responses were close to zero, as depicted. Both a- and b- waves were irreversible.

In the third experimental group, which was administered EA (group III); a notable enhancement in ERG values was observed within the corresponding time range. The results show a significant increase ($P<0.05$) in a- and b-wave amplitude and a decrease in implicit time. The percentage difference in a-wave was 70% in its amplitude and 67% in its implicit time, whereas the percentage difference in b-wave was 78% and 87.1% for its amplitude and implicit time, respectively. The a-wave is more affected than the b-wave. Over time, improvement can be increased.

Apoptosis

DNA fragmentation

Agarose gel electrophoresis analysis of retinal DNA fragmentation after intravitreal administration of SI, showed a gradual emergence of the ladder pattern associated with internucleosomal fragmentation from multiple time points. This pattern is a hallmark of MD model apoptosis. A barely visible ladder pattern was seen at 7 days. However, the band intensity peaked 21 days after injection. No DNA ladder was present in the control retina (control). In the group treated with EA, the bands decreased gradually (Fig. 3).

Table 2 illustrates the number of bands as bp and percentage of bp in each band for ladder in all groups, control, MD model and which was treated with EA compared with control retina. As shown in the table, the ladder reflects 10 bands with different percentages in contrast to the control of that lake of the DNA ladder. Seven days after SI injection, nine bp

Table 1 The mean and standard deviation of the amplitude and implicit time of the a-and b-waves of electroretinogram in all rabbits groups

		7 days		14 days		21 days	
ERG waves	Group I (Control)	Group II (SI group)	Group III (SI+EA)	Group II (SI group)	Group III (SI+EA)	Group II (SI group)	Group III (SI+EA)
a-wave							
msec	13.26 ± 0.92^{a}	16.25 ± 0.96^{b}	15.2 ± 0.16^{b}	18.15 ± 0.5^{c}	15.37 ± 0.96^{b}	18.31 ± 0.31^{c}	14 ± 0.82^{a}
μV	26.1 ± 1.9^{a}	2.35 ± 2.9^{b}	8 ± 0.9^{c}	1.3 ± 0.8^{b}	8 ± 1.2^{c}	1.1 ± 1.1^{b}	10 ± 1.5^{c}
b-wave							
msec	34 ± 0.69^{a}	38.1 ± 2.20^{b}	38.4 ± 0.49^{b}	40 ± 2.31^{b}	36 ± 1.79^{b}	40 ± 2.83^{b}	38.2 ± 2.1^{b}
μV	54.8 ± 1.81^{a}	4.91 ± 2.14^{b}	20.4 ± 1.1^{c}	1.5 ± 0.91^{b}	20.20 ± 1.9^{c}	1.4 ± 0.41^{b}	22 ± 1.81^{c}

All data with a different superscript letter (a, b, c) in the same raw are significantly different at P value less than 0.05, using analysis of variance test.

Figure 3

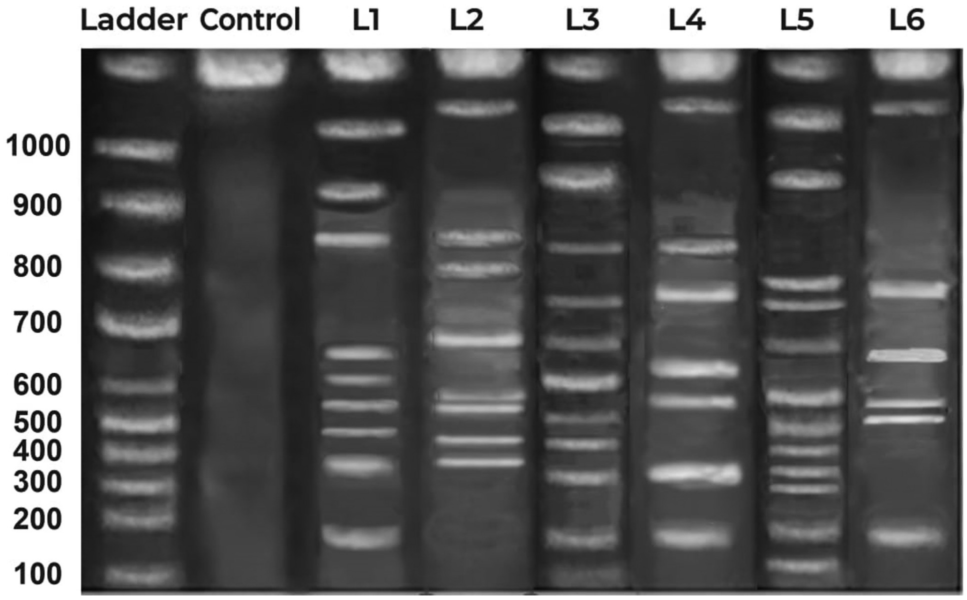

DNA fragmentation analysis by gel electrophoresis. The retinal samples from control, received SI and received SI and EA throughout 7 (L1 and L2), 14 (L3 and L4) and 21 (L5 and L6) days. The ladder pattern of nonrandom internucleosomal cleavage was displayed at all-time points. The first column is the marker (100 bp).

fragmentations (180, 360, 407.98, 540, 616.46, 651, 843.55, 905.08, and 1008.23 bp) appeared in the MD model. The fragmentations were increased for 12 bp bands up to 21 days of intravitreal injection of SI. In the group treated with EA, the results revealed a decrease of fragmented bands that were 8, 7, and 6 bands for 7, 14, and 21 days, respectively.

Caspase-3 and caspase-7 activity

Caspase-3 and caspase-7 are known key molecules in the process of apoptosis, playing an important role in the execution of apoptosis. The concentration of caspase-3 and caspase-7 activity was 1.289±0.12 ng/mg protein and 0.291±0.03 ng/mg protein, respectively, for the control group, as shown in Table 3. A statistically significant ($P \leq 0.05$) increase of caspase-3 and −7 activity was observed after 7 days due to intravitreal injection of SI. The maximum increase of relative caspase-3 and −7 activities was 9.756±0.67 ng/mg protein and 3.529±0.24 ng/mg protein, respectively, which appeared after 21 days. On the other hand, there was a significant decrease ($P \leq 0.05$) in both caspase activities for all groups administrated EA.

Table 2 Bands and percentage of bp fragmentation for ladder and different groups compared with control

					7 days				14 days				21 days			
	Ladder		Group I (Control)		Group II (SI group)		Group III (SI + EA)		Group II (SI group)		Group III (SI+EA)		Group II (SI group)		Group III (SI +EA)	
Band NO.	bp	%	bp	%	bp	%	bp	%	bp	%	bp	%	bp	%	bp	%
1	1000	11.59	1002	100	1008.23	21.58	1020.11	24.53	1017.34	17.9	1074	47.04	1023.51	10.52	1074	47.34
2	900	13.74	–	–	905.08	3.89	908.07	5.42	919.28	3.85	815	9.90	910.02	3.34	748	3.83
3	800	13.03	–	–	843.55	4.26	800.44	6.14	820.54	5.71	720	7.49	790.61	4.62	654	4.31
4	700	14.38	–	–	651.94	5.21	660	8.35	720	10.13	637	11.30	720	5.46	540	14.68
5	600	6.66	–	–	616.46	7.36	530.43	15.41	671.16	9.62	540	5.80	670.8	6.9	360	16.69
6	500	8.4	–	–	540	13.92	540	13.21	626.72	8.12	360	11.34	540	16.36	180	13.15
7	400	11.66	–	–	407.98	11.41	407.98	12.41	540	13.04	180	7.13	500	5.33	–	–
8	300	7.23	–	–	360	12.66	360	14.60	416.02	7.73	–	–	410.34	7.25	–	–
9	200	6.88	–	–	180	14.7	–	–	360.2	11.5	–	–	360	15.21	–	–
10	100	6.43	–	–	–	–	–	–	180	12.1	–	–	320	7.10	–	–
11	–	–	–	–	–	–	–	–	–	–	–	–	180	12.1	–	–
12	–	–	–	–	–	–	–	–	–	–	–	–	110.92	5.81		
Total		10			9	100	8	100	10	100	7	100	12	100	6	100

Table 3 Caspase-3 and 7 levels in retina tissue of rabbits groups after 7, 14, and 21 days of SI injection and EA treatment

		7 days		14 days		21 days	
	Control group I	SI group II	Pom. group III	SI group II	Pom. group III	SI group II	Pom. group III
Cas.3 ng/mg protein	1.289±0.12[a]	9.756±0.67[b]	8.314±0.31[b]	11.469±0.82[b]	7.28±0.36 [c]	13.342±0.91[d]	7.053±0.35[c]
Cas.7 ng/mg protein	0.291±0.03[a]	3.529±0.24[b]	3.064±0.15[b]	3.911±0.41[b]	3.087±0.16[b]	4.531±0.62[b]	3.135±0.22[b]

All data with a different superscript letter (a, b, c, d) in the same raw are significantly different at *P* value less than 0.05, using analysis of variance test.

Discussion

MD is an ophthalmic neurodegenerative disease that causes permanent vision loss in people worldwide [2]. In the context of MD, the pathological mechanism leads to the dysfunction and impairment of the retinal pigmented epithelium and photoreceptors located in the macula [14]. More studies suggest that (in MD) RPE, photoreceptors, and inner nuclear layer cells die by apoptosis [18–20]. Only a few medications are available to slow the disease's progression, and there is no known cure for the neural retina's degeneration [2]. The neurodegenerative process associated with MD is characterized by the involvement of oxidative stress. Therefore, using antioxidants is likely beneficial, as evidenced by the observed reduction in both the occurrence and advancement of MD. The literature has documented the utilization of dietary antioxidants that are readily accessible and administered through natural means [2]. In this study, we reported the efficiency of EA as a potent antioxidant supplement in reducing the prevalence and progression of MD. EA is a reliable source of many antioxidants. It is recognized as a naturally occurring polyphenolic compound that is bioactive and pharmacologically effective, protecting cells from free radical damage [21]. Hence, alternative preventive and/or treatment approaches are required.

To further support the validity of this research, fundus photographs, ERGs, and apoptosis recordings were used to evaluate it clinically.

A close fundus examination detected visible Fundus changes to the naked eye in the second and the third group. Attenuation of chorioretinal vasculature was identified. Our results agree with previous work [15–22] on subtle changes caused by SI toxicity (group 2). There is a correlation exists between the observed alterations in retinal vessels and the progression of MD as proposed by Taylor *et al.* [23]. The majority of the evidence, the author underlines, points to a decline in vessel density in the superficial vascular complex of the retina in people with early to moderate MD. However, it is important to exercise caution when interpreting these studies due to the inconsistent methodologies and terminology employed across different research investigations.

ERGs are commonly employed to evaluate the functionality of photoreceptors and inner retinal processes [24]. The findings of our study revealed that the ERG obtained from the control animals exhibited the presence of two widely recognized waves, the a-wave, and b-wave, serving as indicators for assessing retinal function. The activity of the photoreceptor is denoted by the a-wave. The b-wave is generated in the inner retinal layer, where the retinal circulation is the principal blood supply. It can be asserted that the amplitude of the b-wave is influenced by various factors, including the a-wave, retinal circulation, and the dynamic interplay between the generators of the a-wave and b-wave [25–27]. The findings of our study indicate that the MD model had a significant impact on all ERG parameters, suggesting notable functional alterations in each parameter. The amplitudes of a- and b- waves were significantly reduced, and their implicit time increased. The most significant decrease appeared on the 21-day mark; a- and b-wave responses were near zero. The findings mentioned above were consistent with the conclusions drawn by various authors [15,28–30]. SI is considered a ROS inducer and an oxidative toxic agent that has a destructive effect on RPE cells and photoreceptors. Oxidative stress is a major factor contributing to MD. Thus, this makes SI a reproducible model of MD [24,31]. The overabundance of ROS has the potential to cause damage to cellular proteins, lipids, and DNA, leading to severe lesions within cells that can be fatal [32]. Consequently, ERG must be affected.

In addition, to further clarify, the present findings show an increased incidence of retinal cell death and DNA fragmentation, associated with a significant increase in caspase-3 and caspase-7 levels in rabbit retinal tissues in the MD model. Our results agree with previous studies [33–37]. The increased prevalence of apoptosis observed in the retinal tissues of rabbits provided evidence for the existence of oxidative stress in the context of subarachnoid hemorrhage.

ROS plays crucial roles in various types of cellular demise, including apoptosis, ferroptosis, and necroptosis. Lipid peroxidation, which is facilitated by ROS, is widely acknowledged as a significant mechanism responsible for the degradation and impairment of cellular membranes. Moreover, it has been proposed that lipid peroxidation contributes to the progression of tissue damage. Tissues with a high proportion of membrane lipids exhibit a heightened concentration of tissue oxygen and are particularly susceptible to impairment caused by oxidative stress. Additionally, the retina presents elevated levels of polyunsaturated fatty acids, which enhance its susceptibility to oxidative damage and lipid peroxidation of cellular membranes, leading to cell death through either apoptosis or necrosis [38,39]. The process of apoptosis is regarded as the mechanism by which photoreceptors undergo destruction [15]. This particular mode of cellular demise has been associated with numerous physiological and pathological states [40,41]. Apoptosis is characterized by three significant processes: the activation of protease enzymes, the degradation of DNA, and the phagocytosis of apoptotic bodies by neighbouring cells. Caspases are proteases that specifically target cysteine and aspartate residues, and they play a pivotal role in orchestrating and carrying out the apoptotic process in various apoptotic systems [42]. There are two main pathways for activating caspases, which degrade vital survival proteins. The extrinsic pathway begins when ligands bind to death receptors. Another pathway, the intrinsic pathway, releases cytochrome c from mitochondrial intermembrane space into the cytosol [40,43].

Caspase-3 is a well-established pivotal molecule in the mechanism of programmed cell death, known as apoptosis, and is significantly involved in the execution phase of this process. Numerous studies have indicated a strong correlation between the activation of caspase-3 and the apoptosis occurrence. Specifically, retinal damage can trigger apoptosis in cells located in the pigment epithelial, outer nuclear layer, and ganglion cells due to retinal damage [44,45].

Caspase-7 functions as an effector enzyme in initiating apoptosis, following its cleavage and activation by initiator caspases, such as caspase-1 [46]. The enzyme's active site includes a catalytic cysteine residue that facilitates the cleavage of diverse substrates. The primary role of caspase-7 is to facilitate the generation of ROS and contribute to the process of cell detachment in the context of apoptosis [47,48]. The observed rise in apoptosis rates is evidence of oxidative stress within the retinal tissues of the rabbit model of MD.

Consequently, the rabbits that received EA exhibited a notable amelioration in the adverse effects. The enhancement was noted across all ERG and apoptosis indicators, although the reduction in chorioretinal vasculature remained evident. Based on the observations mentioned above, one can infer that the EA treatment exhibits significant efficacy.

The polyphenolic structure of EA is primarily responsible for its antioxidant capacity [41,49–51]. EA's two lactones and four hydroxyl groups allow it to scavenge a broad range of ROS. While EA can deactivate peroxyl radicals, hydroxyl radicals, nitrogen dioxide, and peroxynitrite in aqueous solution at physiological pH [52,53], it can better scavenge ROS than reactive nitrogen species [54]. Because of its expected ability to regenerate and not be reduced after metabolism, EA is thought to be an exceptional protector against oxidative stress. This means that this polyphenolic compound can continue to provide protection even at low concentrations [21].

Polyphenols have both direct and indirect antioxidant activities, which are essential in understanding why EA has been identified as a potent antioxidant. The process of donating an electron or hydrogen atom directly can lessen the harmful effects of free radicals. Moreover, the presence of a highly conjugated system and specific hydroxylation patterns is considered a significant factor in contributing to antioxidant activities. The formation of free radicals is suppressed by polyphenols, which lowers the rate of oxidation. This is achieved by inhibiting both the formation and deactivation of active species and precursors associated with free radicals. Polyphenols act directly as radical scavengers within the lipid peroxidation chain reactions and effectively break the chain. They provide an electron to the unpaired electron of the free radical, which can neutralize both radicals. Consequently, the chain-breaking agents transform into stable radicals with reduced reactivity, effectively halting the progression of the chain reactions [55–58]. That may explain the improvement of ERG; this agrees with Raghu *et al.* [12]. Polyphenols are recognized for their radical scavenging abilities and their capacity to act as metal chelators. Chelating transition metals, such as Fe^{2+}, can effectively decrease the rate of the Fenton reaction, thereby mitigating the oxidation induced by the highly reactive hydroxyl radicals [57,58]. The retina is susceptible to iron imbalance, the occurrence of iron overload in the retina leads to the generation of a significant quantity of ROS. This will aggravate local oxidative stress and inflammatory reactions and even lead to ferroptosis, eventually resulting in retinal dysfunction [59]. Polyphenols do not exert their effects in isolation. Recent research has revealed that polyphenols can act as co-antioxidants, thereby contributing to the regeneration of crucial vitamins [60].

In addition to the aforementioned potential mode of antioxidant actions, it is also noteworthy to consider other indirect significant mechanisms, including the inhibition of xanthine oxidase and the elevation of endogenous antioxidants [61]. EA can stimulate the production of antioxidant enzymes, including glutathione peroxidase, catalase, and superoxide dismutase. These enzymes are essential for decomposing toxic materials such as hydrogen peroxide, hydroperoxides, and superoxide anions. The depletion of GSH in the retina causes the death of RPE and subsequent death of photoreceptors has been observed in MD [62]. That may explain the enhancement of apoptosis indicators. Additionally, EA has been found to suppress the activity of enzymes like xanthine oxidase [63].

Conclusion

The present study provides that $NaIO_3$ creates an excellent MD model. Moreover, the study sheds new light suggesting implementing an alternative treatment regimen involving the use of EA as a protective measure for the retina. The administration of EA demonstrated a notable impact in improving the retina's function, and the apoptosis decreased. It is noted that the organic nature of the EA is a distinguishing feature. Hence, employing it as a therapeutic intervention allows for avoiding synthetic compounds, a preference that arises due to the potential for severe toxicity. Further investigations are required in this preclinical study to elucidate the mechanism of action of the bioactive ingredients and fully uncover the potential of EA as both a preventive and therapeutic agent, as well as to determine the potential effect in reducing chronic inflammation.

Financial support and sponsorship

This study has been supported by the Visual Science Department, Research Institute of Ophthalmology, Giza, Egypt.

Conflicts of interest

There are no conflicts of interest.

References

1 Monika F, Thomas G, Robyn H, Usha C, Steffen S, Caroline C, Wai T, *et al.* Age-related macular degeneration. Nature Reviews Disease Primers 2021; 7:31.

2 Dziedziak J, Kasarełło K, Cudnoch J, Edrzejewska A. Dietary Antioxidants in Age-Related Macular Degeneration and Glaucoma. Antioxidants 2021; 10:1743.

3 Usategui-Martin R, Fernandez-Bueno I. Neuroprotective therapy for retinal neurodegenerative diseases by stem cell secretome. Neural Regen Res 2021; 16:117–118.

4 Irina M, Samo R, Borut P. Antioxidant Vitamins and Ageing. In: Harris J, Korolchuk V (eds). Biochemistry and Cell Biology of Ageing: Part I Biomedical Science. Subcellular Biochemistry. Singapore: Springer 2018; 90:1–25.

5 Valko M, Leibfritz D, Moncol J, Cronin M.T., Mazur M, Telser J. Free radicals and antioxidants in normal physiological functions and human disease. Int J Biochem Cell Bio 2007; 39:44–84.

6 Evans JR, Lawrenson JG. Antioxidant vitamin and mineral supplements for slowing the progression of age-related macular degeneration. Cochrane Database Syst Rev 2017; 7:CD000254.

7 Chapman N, Jacobs R, Braakhuis A. Role of diet and food intake in age-related macular degeneration: A systematic review. Clin Exp Ophthalmol 2019; 47:106–127.

8 Deepika Maurya P. Ellagic acid: insight into its protective effects in age-associated disorders. 3 Biotech 2022; 12:340.

9 Zhang Z, Liu N, Sun M. Research Progress of Immunotherapy for Gastric Cancer. Technol Cancer Res Treat 2023; 22:153303382211 50555.

10 Guendalina Z, Sara B, Giorgia A, Federica T, Silvana A, Gabriele C. Review: Formulation Strategies to Improve Oral Bioavailability of Ellagic Acid. Appl. Sci. 2020; 10:3353.

11 Zhipeng L, Hongli Y, Chaolong L, Changduo W, Xianhu Z, Jianqin Y, *et al.* Efficiency co-delivery of ellagic acid and oxygen by a non-invasive liposome for ameliorating diabetic retinopathy. Int J Pharm 2023; 641: 122987.

12 Raghu G, Akileshwari C, Reddy V, Reddy G. Attenuation of diabetic retinopathy in rats by ellagic acid through inhibition of AGE formation. J Food Sci Technol 2017; 54:2411–2421.

13 Chader G. Animal models in research on retinal degenerations: past progress and future hope. Vis Res 2002; 42:393–399.

14 Kocab A, Bacellar-Galdino M, Zacks D, Jamison J, Van De Goor J. Inhibition of Fas with ONL 1204 provides protection in a novel rabbit model of dry AMD. ARVO annual meeting 2020. Poster presentation. https://experimentica.com/model_inner/sodium-iodate-retinal-degeneration

15 Bum-Joo C, Jong-Mo S, Hyeong G, Hum C. Monocular retinal degeneration induced by intravitreal injection of sodium iodate in rabbit eyes. Jpn J Ophthalmol 2016; 60:226–237.

16 Marmor T, Freeman R, Okma K. Comparative Studies and the Politics of Modern Medical Care. New Haven, CT, USA: Yale University Press; 2009. https://doi.org/10.12987/9780300155952

17 Marmor M, Fulton A, Holder G, Miyake Y, Brigell M, Bach M. ISCEV Standard for full-field clinical electroretinography. Doc Ophthalmol 2009; 118:69–77.

18 Somasundaran S, Constable I, Mellough C, Carvalho L. Retinal pigment epithelium and age-related macular degeneration: A review of major disease mechanisms. Clin Exp Ophthalmol 2020; 48:1043–1056.

19 Man S, Karki R, Kanneganti T. Molecular mechanisms and functions of pyroptosis, inflammatory caspases and inflammasomes in infectious diseases. Immunol Rev 2017; 277:61–75.

20 Dunaief J, Dentchev T, Ying G, Milam A. The role of apoptosis in age-related macular degeneration. Arch Ophthalmol 2002; 120:1435–1442.

21 Javad S, Cristina Q, Carla M, Rodrigo C, Marco A, Alexandr P, *et al.* Review Article, Ellagic Acid: A Review on Its Natural Sources, Chemical Stability, and Therapeutic Potential. Oxid Med Cell Longev 2022; 2022: 3848084.

22 Zhou P, Kannan R, Spee C, Sreekumar P, Dou G., David R. Protection of Retina by αB Crystallin in Sodium Iodate Induced Retinal Degeneration. PLOS ONE 2014; 9:e98275.

23 Taylor TRP, Menten MJ, Rueckert D, Sivaprasad S, Lotery AJ. The role of the retinal vasculature in age-related macular degeneration: a spotlight on OCTA. Eye (Lond) 2024; 38:442–449.

24 Huang W, Liu P, Wang N. Electroretinogram (ERG) to Evaluate the Retina in Cases of Retinitis Pigmentosa (RP) In: Tsang SH, Quinn PM, (eds). Retinitis Pigmentosa. Methods in Molecular Biology. New York, NY: Humana; 2023; 2560:111–122.

25 Stone WL, Patel BC, Basit H, *et al.* Retinopathy. [Updated 2023 Aug 8]. In: StatPearls [Internet]. Treasure Island (FL): StatPearls Publishing; 2024 Jan-. Available from: https://www.ncbi.nlm.nih.gov/books/NBK541131/

26 Rodriguez S. Electroretinogram. Eye wiki 2023. https://eyewiki.aao.org/Electroretinogram

27 Kolb H, Nelson R, Fernandez E, Jones B. Review: Facts and Figures Concerning the Human Retina quoted from Web vision: The Organization of the Retina and Visual System. Salt Lake City (UT): University of Utah Health Sciences Center; 2005.

28 Céline K, Koen T, Jacoline B, Colby F, Boris V, Kapil B, Arthur A. Sodium-iodate injection can replicate retinal degenerative disease stages in pigmented mice and rats: non-invasive follow-up using OCT and ERG. Int J Mol Sci 2022; 23:2918.

29 Hamid A, Taki T, Narsis D, Hamid A, Hossein Z, Taher T. Histological and Electrophysiological Changes in the Retinal Pigment Epithelium after Injection of Sodium Iodate in the Orbital Venus Plexus of Pigmented Rats. J Ophthalmic Vis Res 2016; 11:170–77.

30 Franco L, Zulliger R, Wolf-Schnurrbusch U, Katagiri Y, Kaplan H, Wolf S. Decreased visual function after patchy loss of retinal pigment epithelium induced by low-dose sodium iodate. Invest Ophthalmol Vis Sci 2009; 50:4004–10.

31 Chi-Ming C, Duen-Yi H, Ponarulselvam S, Shu-Hao H, Wan-Wan L. Reactive oxygen species-dependent mitochondrial dynamics and autophagy confer protective effects in retinal pigment epithelial cells against sodium iodate induced cell death. J Biomed Sci 2019; 26:40.

32 Dan L, Zongxian D, Kaili D, Xiangshi Y, Shixue C. Reactive Oxygen Species as a Link between Antioxidant Pathways and Autophagy. Oxid Med Cell Longev 2021; 2021:5583215.

33 Olivares-González L, Velasco S, Campillo I, Rodrigo R. Retinal Inflammation, Cell Death and Inherited Retinal Dystrophies. Int J Mol Sci 2021; 22:2096.

34 Mao X, Pan T, Shen H, Xi H, Yuan S, Liu Q. The rescue effect of mesenchymal stem cell on sodium iodate-induced retinal pigment epithelial cell death through deactivation of NF-kappaB-mediated NLRP3 inflammasome. Biomed Pharmacother 2018; 103:517–523.

35 Hanus J, Anderson C, Sarraf D, Ma J, Wang S. Retinal pigment epithelial cell necroptosis in response to sodium iodate. Cell Death Discov 2016; 2:16054.

36 Juel H, Faber C, Svendsen S, Vallejo A, Nissen M. Inflammatory cytokines protect retinal pigment epithelial cells from oxidative stress induced death. PLoS ONE 2016; 8:e64619.

37 El-Sayyad H, El-Sherbiny M, Sobh M, Abou-El-Naga A, Ibrahim M, Mousa S. Protective effects of morus alba leaves extract on ocular functions of pups from diabetic and hypercholesterolemic mother rats. Int J Biol Sci 2011; 7:715–728.

38 Eman A, Amal E. Apoptosis and electroretinogram after intravitreal injection of methotrexate in an experimental rabbit model. Gen Physiol Biophys 2016; 35:231–236.

39 Ayala A, Muñoz MF, Argüelles S. Lipid peroxidation: production, metabolism, and signaling mechanisms of malondialdehyde and 4-hydroxy-2-nonenal. Oxid Med Cell Longev 2014:360438.

40 Gloria E, Spencer B. Reactive Oxygen Species (ROS) Regulates Different Types of Cell Death by Acting as a Rheostat. Oxid Med Cell Longev 2021; 2021:9912436.

41 Francesca D, Lynnette R. Could Pomegranate Juice Help in the Control of Inflammatory Diseases? Review Nutrients 2017; 9:958.

42 Chang H, Yang X. Proteases for cell suicide: functions and regulation of caspases. Microbiol Mol Biol Rev 2000; 64:821–846.

43 Perche O, Doly M, Ranchon-Cole I. Caspase-dependent apoptosis in light-induced retinal degeneration. Invest Ophthalmol Vis Sci 2007; 48:2753–2759.

44 Marzieh A, Saeed T, Elina K, Omid V, Mortaza T, Mahshid T, *et al.* Caspase-3: Structure, function,and biotechnological aspects. Biotechnol Appl Biochem 2022; 69:1633–1645.

45 Tian X, Zhu Y. Apoptosis of rabbit retinal cell after eyeball rupture. Asian Pac J Trop Med 2013; 6:273–279.

46 Julien O, Wells JA. Caspases and their substrates. Cell Death Differ 2017; 24:1380–1389.

47 Kashyap D, Garg VK, Goel N. Intrinsic and extrinsic pathways of apoptosis: Role in cancer development and prognosis. Advances in protein chemistry and structural biology. 2021; 125:73–120. https://doi.org/10.1016/bs.apcsb.2021.01.003

48 Brentnall M, Rodriguez-Menocal L, De Guevara R, Cepero E, Boise L. Caspase-9, caspase-3 and caspase-7 have distinct roles during intrinsic apoptosis. BMC Cell Biology 2013; 14:32.

49 Kábelová A, Malínská H, Marková I, Oliyarnyk O, Chylíková B, Šeda O. Ellagic Acid Affects Metabolic and Transcriptomic Profiles and Attenuates Features of Metabolic Syndrome in Adult Male Rats. Nutrients 2021; 13:804.

50 Aida Z, Sedigheh A, Shaghayegh H. Potent health effects of pomegranate. Adv Biomed Res 2014; 3:100.

51 Gil M, Tomás Barberán F, Hess Pierce B, Holcroft D, Kader A. Antioxidant activity of pomegranate juice and its relationship with phenolic composition and processing. J Agric Food Chem 2000; 48:4581–4589.

52 Galano A, Francisco M, Perez-Gonzalez A. Ellagic acid: an unusually versatile protector against oxidative stress. Chem Res Toxicol 2014; 27: 904–918.

53 Priyadarsini I, Khopde S, Kumar S, Mohan H. Free radical studies of ellagic acid, a natural phenolic antioxidant. J Agric Food Chem 2002; 50:2200–2206.

54 Tiwari M, Mishra P. Modeling the scavenging activity of ellagic acid and its methyl derivatives towards hydroxyl, methoxy, and nitrogen dioxide radicals. J Mol Model 2013; 19:5445–5456.

55 Alberto B, Marco B, Maddalena C, Giulia B, Giorgio C, Elisabetta M. Polyphenols: From Theory to Practice. Foods 2021; 10:2595.

56 Rodríguez-Morató J, Robledo P, Tanner J, Boronat A, Pérez-Mañá C, Chen C, *et al.* CYP2D6 and CYP2A6 biotransform dietary tyrosol into hydroxyty. Food Chem 2017; 217:716–725.

57 Soldevila-Domenech N, Boronat A, Mateus J, Diaz-Pellicer P, Matilla I, Pérez-Otero M, *et al.* Generation of the Antioxidant Hydroxytyrosol from Tyrosol Present in Beer and Red Wine in a Randomized Clinical Trial. Nutrients 2019; 11:2241.

58 Governa P, Manetti F, Miraldi E., Biagi M. Effects of in vitro simulated digestion on the antioxidant activity of different Camellia sinensis (L.) Kuntze leaves extracts. Eur Food Res Technol 2022; 248:119–128.

59 Li Y, Cheng Z, Luo T, Lyu H. Therapeutic potential of iron chelators in retinal vascular diseases. Int J Ophthalmol 2023; 16:1899–1910.

60 Yao H, Li C, Chang C. Epigallocatechin-3-Gallate Reduces Hepatic Oxidative Stress and Lowers CYP-Mediated Bioactivation and Toxicity of Acetaminophen in Rats. Nutrients 2019; 11:1862.

61 Seki H, Akiyoshi T, Imaoka A. Inhibitory kinetics of fruit components on CYP2C19 activity. Drug Metab Pharmacokinet 2019; 34:181–186.

62 Sun Y, Zheng Y, Wang C, Liu Y. Glutathione depletion induces ferroptosis, autophagy, and premature cell senescence in retinal pigment epithelial cells. Cell Death Dis 2018; 9:753.

63 Chang T, Chen J, Lee W. Differential inhibition and inactivation of human CYP1 enzymes by trans-resveratrol: Evidence for mechanism-based inactivation of CYP1 A2. J Pharmacol Exp Ther 2001; 299:874–882.